

**Dedication in honour of  
Allan Sandage**

# Allan Sandage and the distance scale

G. A. Tammann and B. Reindl

Department of Physics and Astronomy, University of Basel, Klingelbergstrasse 82, 4056 Basel, Switzerland

email: g-a.tammann@unibas.ch

**Abstract.** Allan Sandage returned to the distance scale and the calibration of the Hubble constant again and again during his active life, experimenting with different distance indicators. In 1952 his proof of the high luminosity of Cepheids confirmed Baade's revision of the distance scale ( $H_0 \sim 250 \text{ km s}^{-1} \text{ Mpc}^{-1}$ ). During the next 25 years, he lowered the value to 75 and 55. Upon the arrival of the *Hubble Space Telescope*, he observed Cepheids to calibrate the mean luminosity of nearby Type Ia supernovae (SNe Ia) which, used as standard candles, led to the cosmic value of  $H_0 = 62.3 \pm 1.3 \pm 5.0 \text{ km s}^{-1} \text{ Mpc}^{-1}$ . Eventually he turned to the tip of the red giant branch (TRGB) as a very powerful distance indicator. A compilation of 176 TRGB distances yielded a mean, very local value of  $H_0 = 62.9 \pm 1.6 \text{ km s}^{-1} \text{ Mpc}^{-1}$  and shed light on the streaming velocities in the Local Supercluster. Moreover, TRGB distances are now available for six SNe Ia; if their mean luminosity is applied to distant SNe Ia, one obtains  $H_0 = 64.6 \pm 1.6 \pm 2.0 \text{ km s}^{-1} \text{ Mpc}^{-1}$ . The weighted mean of the two *independent* large-scale calibrations yields  $H_0 = 64.1 \text{ km s}^{-1} \text{ Mpc}^{-1}$  within 3.6%.

**Keywords.** cosmological parameters, distance scale

---

## 1. Introduction

Allan Sandage (1926–2010) was one of the best observers ever, but his driver was always the physical understanding of astronomical phenomena. Physics as his primary goal is exemplified in his ground-breaking paper, *'The ability of the 200-inch Telescope to discriminate between selected World Models'* (1961) that became the basis of modern observational cosmology. Other examples are the emerging understanding of stellar evolution (Sandage & Schwarzschild 1952), the theory of stellar pulsation (Sandage 1958a; Sandage *et al.* 1999), the formation of the Galaxy (Eggen, Lynden-Bell, & Sandage 1962) and of other galaxies (Sandage 1986), including their violent stages (Burbidge, Burbidge, & Sandage 1963), the nature of the expansion field (Humason, Mayall, & Sandage 1956; Sandage 1975; Sandage *et al.* 2010), and the age dating of stellar clusters (e.g., Sandage 1958b) as well as of the Universe (e.g., Sandage 1970, 1972). He devoted several papers to the Tolman test of the nature of redshifts (e.g., Sandage 2010) and he is the father of what has become known as the Sandage–Loeb effect (Sandage 1962a).

Walter Baade, the thesis adviser of Sandage, gave him a tough training in the ancient and intricate art of observing; it was later described in Sandage's outstanding history, *'The Mount Wilson Observatory'* (2004). Soon Sandage excelled himself in that high art and was commissioned to observe also for Hubble. He loved to observe on Mount Wilson and Palomar Mountain. After the split of the Carnegie Institution and the California Institute of Technology in 1980, he did not go to Palomar again. On Mount Wilson he was one of the last observers before the Mountain was given into other hands in the mid-1980s. A consolation became the wide-field 2.5 m telescope of the Las Campanas Observatory, where he took many direct plates for his atlases and for the extensive Virgo Cluster survey (Sandage *et al.* 1985). In total, he spent more than 2000 nights at various

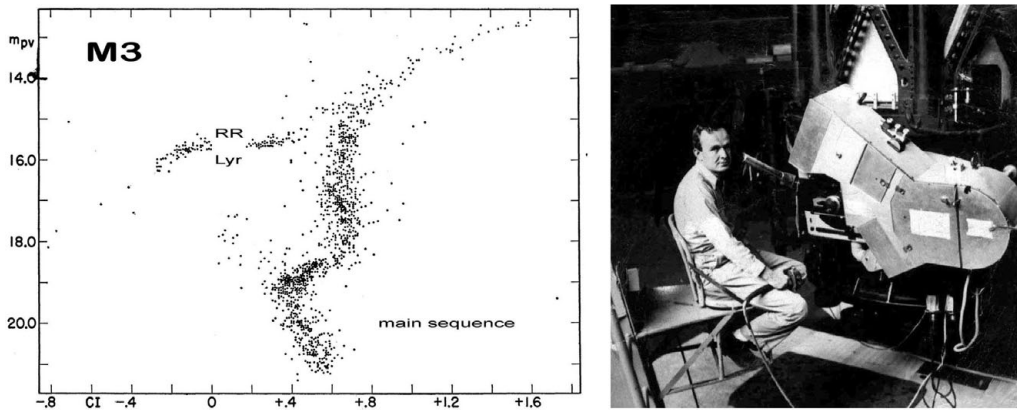


**Figure 1.** (left) Color–magnitude diagram (CMD) of the globular cluster M3 from Sandage’s thesis, where he matched the cluster main sequence with the main sequence of the young Population I, showed the locus of RR Lyrae stars, and discussed the influence of metallicity on the CMD. (right) Allan Sandage at the spectrograph of the Mount Wilson 60 inch telescope in 1950.

telescopes. He felt a strong responsibility to reduce and publish the enormous amount of accumulated observations. After 1990 he used only the *Hubble Space Telescope (HST)*; it was Abhijit Saha who introduced him to the novel technique of CCD photometry.

## 2. Early Work

His thesis assignment was the color–magnitude diagram (CMD) of the globular cluster M3. By pushing the photometry down to an unprecedented limit of 23<sup>rd</sup> mag, he could find the cluster’s main sequence and fit it to the main sequence of the young Population I (Fig. 1; Sandage 1953). This provided an essential clue to the theory of stellar evolution, but at the same time it solved a long-standing problem of the distance scale. Baade (1944) had pointed out that galaxy distances derived from RR Lyrae stars and Cepheids were in contradiction. It became now clear that the RR Lyrae calibration was roughly correct, whereas the Cepheids were too faint by  $\sim 1.5$  mag. This confirmed Baade’s (1944) proposal that all of Hubble’s distances had to be doubled. In the following more than 50 years Sandage published some 40 papers on the physics and luminosity of RR Lyrae stars and 50 papers on Cepheids. The distance scale runs like a red line through his entire professional life.

The next stretch came with the paper of Humason *et al.* (1956), for which Sandage had written the analytical part. He much improved Hubble’s galaxy magnitudes and showed that what Hubble had identified as brightest stars in other galaxies were in fact HII regions. This led to  $H_0 = 180 \pm 40 \text{ km s}^{-1} \text{ Mpc}^{-1}$ . Two years later, he (Sandage 1958a) concluded from a re-discussion of the Cepheid distances and from straightening out the confusion of HII regions and brightest stars that  $50 < H_0 < 100 \text{ km s}^{-1} \text{ Mpc}^{-1}$ ; this was an increase of Hubble’s distance scale by a factor of 5 to 10. Sandage (1962b) defended this range of  $H_0$ , also using the angular size of the largest HII regions and novae, against higher values proposed at the influential Santa Barbara Conference on Extragalactic Research.

Determination of the extragalactic distance scale had been described by Baade (1948) as one of the main goals of the forthcoming 200 inch Telescope. Correspondingly, Baade and Hubble had taken repeated photographs, once the telescope had gone into operation, of several galaxies for work on their Cepheids; they were joined by Sandage in the

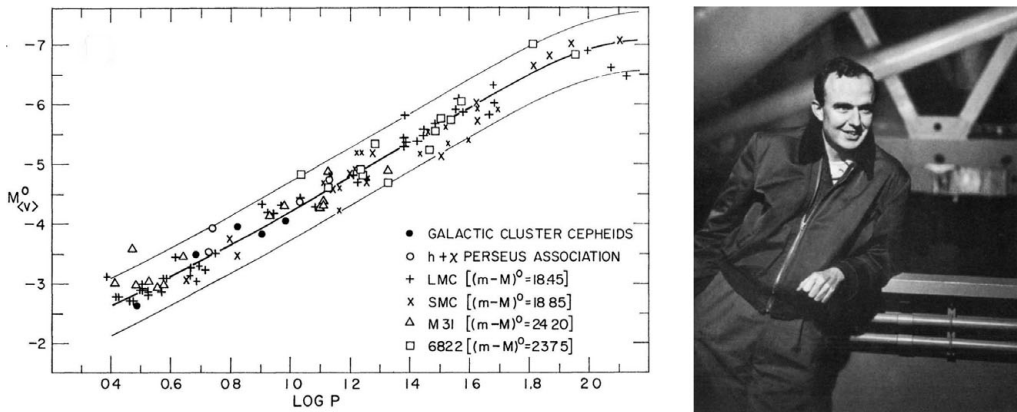


**Figure 2.** (left) The P–L relation in 1968 from a superposition of Cepheids in four galaxies and five Galactic Cepheids with known distances. The resulting distances are marked. (right) Allan Sandage in front of the 200 inch Telescope on Palomar Mountain in 1953.

following years. A parallel task was for Sandage, W. A. Baum, and H. C. Arp to establish reliable photo-electric magnitude sequences in a number of fields. In the mid-1960s, there were sufficient data for Sandage, who had inherited the photographic plates of Baade and Hubble, to start a new onslaught on  $H_0$ .

It was preceded by a new period–luminosity (P–L) relation for Cepheids (Sandage & Tammann 1968), which was a superposition of the known Cepheids in Large and Small Magellanic Clouds (LMC, SMC), M31, and NGC 6822, and whose zero point was based on five Galactic Cepheids that are members of open clusters with known distances (see Fig. 2). The moduli of the LMC and SMC agree with modern values to within 0.1 mag, the modulus of M31, based on the excellent Cepheids of Baade & Swope (1963), was still 0.2 mag short, and the distance to NGC 6822 was too long due to internal absorption. Another prerequisite for the new determination of  $H_0$  was the first Cepheid distance outside the Local Group, i.e. of the highly resolved galaxy NGC 2403 (Tammann & Sandage 1968), which was taken as representative of the whole M81 group.

### 3. The series ‘Steps toward the Hubble Constant’

In the two first steps of the series (Sandage & Tammann 1974–1975), the linear size of the largest HII regions and the luminosity of the brightest blue and red stars were calibrated with the available Cepheid distances. The maximum HII-region size and blue-star luminosity were found to increase with galaxy size, whereas the red-star luminosity is quite stable. In step III, the results were applied to the M101 group which was found at a then surprisingly large distance modulus of  $(m - M) \geq 29.3$  mag, yet in agreement with the modern value (see Section 7). Step IV served to extend and calibrate van den Bergh’s (1960) luminosity classes of spiral and irregular galaxies. These morphological classes depend on the surface brightness and the ‘beauty’ of the spiral structure. In particular, it was found that giant Sc spirals (ScI) have a mean intrinsic face-on luminosity of  $M_{pg} = -21.25 \pm 0.07$  mag. The additional inclusion of fainter luminosity classes gave a Virgo Cluster modulus of  $(m - M) = 31.45 \pm 0.09$  mag, which, with an adopted cluster velocity of  $1111 \text{ km s}^{-1}$ , led to a first hint of  $H_0 = 57 \pm 6 \text{ km s}^{-1} \text{ Mpc}^{-1}$ . To extend the distance scale farther out, remote ScI spirals were selected in the Polar Caps of the National Geographic–Palomar Sky Survey in step VI. For 69 of these galaxies, spectra could be measured, resulting in velocities of  $2700 < v < 21,000 \text{ km s}^{-1}$ . Their apparent

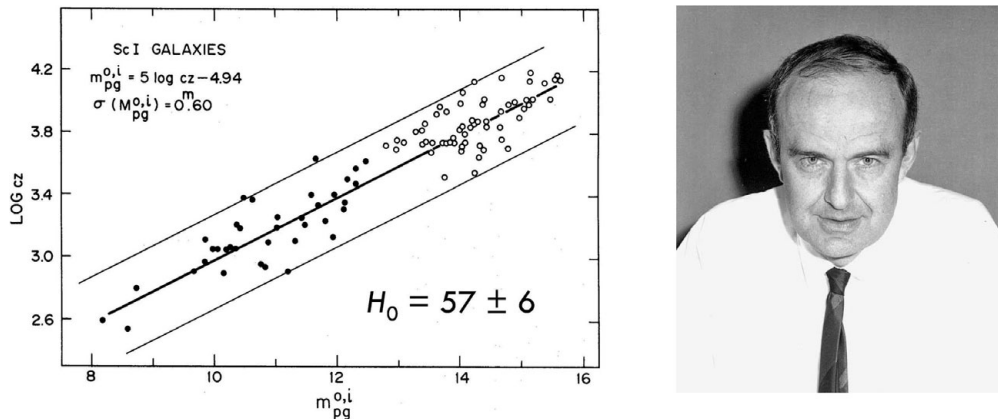


**Figure 3.** (left) Hubble diagram of luminosity class I spirals. Filled symbols are Sc I galaxies from the Shapley–Ames Catalog, open symbols are newly selected Sc I galaxies. Plotted is  $\log v$  versus the corrected Zwicky magnitude. (right) Allan Sandage (1967).

magnitudes,  $m_{pg}$ , were taken from the Zwicky Catalog (Zwicky *et al.* 1961–1968) and corrected for Galactic and internal absorption. The sample out to 15,000 km s<sup>−1</sup> is shown in the Hubble diagram in Fig. 3; it is necessarily biased by the magnitude limit of the catalog. A subsample of 36 galaxies within 8500 km s<sup>−1</sup> was therefore isolated. It was ensured that it was not affected by the magnitude limit. This sample and the above luminosity calibration yields  $H_0 = 56.9$  km s<sup>−1</sup> Mpc<sup>−1</sup> with a statistical error of  $\pm 3.4$  km s<sup>−1</sup> Mpc<sup>−1</sup>.

The summary paper (numbered as step V) gives  $H_0 = 57$  km s<sup>−1</sup> Mpc<sup>−1</sup> with a small statistical error for the global value and with a tacit understanding that the systematic error is on the order of 10%. The *mean* expansion rate of the nearby galaxies was shown not to depend on the Supergalactic longitude and also to be independent of distance, in agreement with an earlier conclusion of Sandage *et al.* (1972). The average random velocity of a nearby galaxy was found to be  $\sim 50$  km s<sup>−1</sup>.

#### 4. Selection Effects

The results of the ‘Steps Toward the Hubble Constant’ met with stiff opposition from G. de Vaucouleurs for the following 10 years. He considered the expansion rate to be a stochastic variable, depending on distance and direction with a mean value of  $90 < H_0 < 110$  km s<sup>−1</sup> Mpc<sup>−1</sup> (e.g., de Vaucouleurs & Peters 1985). The main reason for the disagreement was not that his very local galaxies were  $\sim 0.3$  mag closer than adopted by Sandage and than modern values, but that he did not distinguish between magnitude- and distance-limited samples.

The distinction is decisive in cases where the distance indicator has non-negligible intrinsic scatter, as illustrated in Fig. 4. It shows a Monte Carlo distribution of 500 galaxies randomly distributed within 40 Mpc; their absolute magnitude is  $-18$ , with an intrinsic dispersion of 1 mag. As long as the sample is complete to the given distance limit, their mean luminosity does not change with distance. If the same galaxies are cataloged with a limiting magnitude of  $m = 14$  mag, then the less luminous galaxies are progressively excluded; the rest of the sample has unfortunate statistical properties: the mean luminosity increases with distance, in the present sample by as much as 1 mag and the apparent dispersion decreases with distance. The small dispersion at large distances

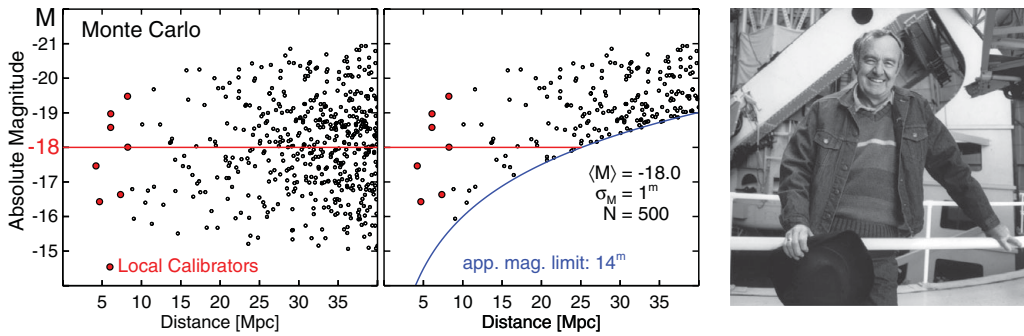


**Figure 4.** (left) Monte Carlo distribution of a galaxy sample with the properties described in the text. (middle) The same distribution, but cut by an apparent-magnitude limit. The mean luminosity of the remaining sample increases with distance. A few local calibrators are shown as open circles. (right) Allan Sandage in front of the 100 inch telescope on Mount Wilson. (*Photo: Douglas Carr Cunningham, 1982*)

has often led to the erroneous conclusion that the true scatter is small and that selection bias was negligible.

Selection bias is particularly dangerous for the Tully–Fisher (T–F) relation because of its large intrinsic scatter of  $\sim 0.5$  mag. Applications of the method to magnitude-limited samples that are not even complete has notoriously led to overestimated values of  $H_0$ . A Hubble diagram of a *distance-limited*, almost complete sample of T–F distances, necessarily limited to  $v_{220} < 1000$  km s $^{-1}$ , gives a local value of  $H_0 = 59 \pm 6$  km s $^{-1}$  Mpc $^{-1}$  (see Fig. 5; Tammann *et al.* 2008b).

Sandage has written a number of papers on various forms of selection bias and its compensation in favorable cases, including a series of 12 papers (e.g., Sandage *et al.* 1995; Sandage 2000).

## 5. The *HST* Project for the Luminosity Calibration of SNe Ia

During the planning phase for *HST*, Sandage formed a small team, including A. Saha, F. D. Macchetto, N. Panagia, and G. A. Tammann, to determine the Cepheid distances of some galaxies with known Type Ia supernovae (SNe Ia), which—with their maximum magnitudes taken as standardizable candles—should lead to a large-scale value of  $H_0$ . In spite of a pilot paper (Sandage & Tammann 1982), the small luminosity dispersion of SNe Ia had not yet been established in 1990 (see Fig. 6, left), but they were proven as exquisite standardizable candles in the following years. The SN *HST* Project was complementary to the *HST* Key Project for  $H_0$  that originally did not include SNe Ia as targets.

The maximum magnitude of SNe Ia must be corrected for internal absorption and standardized to a fixed decline rate  $\Delta m_{15}$  (Phillips 1993). Different procedures have been proposed. We use here the  $m_V^{\text{corr}}$  magnitudes of Reindl *et al.* (2005), because they define a Hubble diagram with a particularly small scatter of 0.14 mag (see Fig. 6, middle) and yield a well-defined intercept of  $C_V = 0.688 \pm 0.004$ . It should be emphasized that the corrected magnitudes of other authors may not have the same zero point because of different choices of intrinsic colors, absorption laws, and reference values of  $\Delta m_{15}$ .

The intercept  $C_V$  of the Hubble line is defined as  $C \equiv \log H_0 - 0.2M - 5$ , hence in the present case,

$$\log H_0 = 0.2\langle M_V^{\text{corr}} \rangle + (5.688 \pm 0.004), \quad (5.1)$$

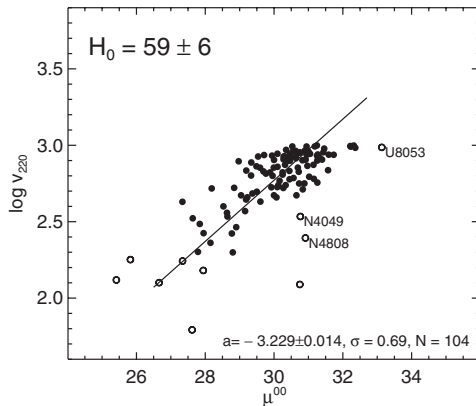


**Figure 5.** (left) Hubble diagram with the T–F distances of an almost complete sample of 104 inclined spiral galaxies within  $1000 \text{ km s}^{-1}$ . (right) Allan Sandage in Baltimore (1988).

where  $\langle M_V^{\text{corr}} \rangle$  is the mean absolute magnitude of SNe Ia. The resulting value of  $H_0$  is the true cosmic value of  $H_0$ , because the Hubble line holds out to  $20,000 \text{ km s}^{-1}$  and can be extended to  $z > 1$  with overlapping data from several SNIa collections (e.g., Hicken *et al.* 2009; Kessler *et al.* 2009).

The SN *HST* Project provided Cepheids in eight SNe Ia-hosting galaxies. Revised period–color and P–L relations allowing for metallicity differences (provided in their latest form for fundamental and overtone pulsators in Tammann *et al.* 2011) were applied to derive Cepheid distances (Saha *et al.* 2006). Combining these distances in the summary paper of the SN *HST* Project, including two additional galaxies from external sources, with the apparent  $m_V^{\text{corr}}$  magnitudes, yields a value of  $\langle M_V^{\text{corr}} \rangle = -19.46 \pm 0.07 \text{ mag}$  and hence with Eq. (5.1),  $H_0 = 62.3 \pm 1.3 \pm 5.0 \text{ km s}^{-1} \text{ Mpc}^{-1}$  (Sandage *et al.* 2006).

The *HST* Key Project found, using the Cepheid distances of eight SNe Ia and barely in statistical agreement,  $H_0 = 71 \pm 2 \pm 6 \text{ km s}^{-1} \text{ Mpc}^{-1}$  (Freedman *et al.* 2001), whereas Riess *et al.* (2011) found from six SNe Ia a significantly higher value of  $H_0 = 73.8 \pm 2.4 \text{ km s}^{-1} \text{ Mpc}^{-1}$ . The divergence of the results depends almost entirely on the different treatment of Cepheids. The latter authors assume the P–L relation of the LMC to be universal and that all color differences of Cepheids with equal periods are caused by internal absorption.

Cepheids are indeed complex distance indicators. Their colors and luminosities depend on metallicities, which are under revision (Bresolin 2011; Kudritzky & Urbaneja 2012), and on the disentangling of metallicity and internal-absorption effects. There are unexplained differences within a given galaxy, and some excessively blue Cepheids suggest the effect of an additional parameter, possibly the helium content (Tammann & Reindl 2012a). Plans to use infrared magnitudes of Cepheids for the SNIa calibration may alleviate some of the problems, but it is obvious that the Cepheid-based calibration needs independent confirmation.

## 6. The Tip of the Red-Giant Branch (TRGB) as a Distance Indicator

Sandage turned to a new distance indicator during his final years: the tip of the red-giant branch (TRGB) as observed in galaxy halos. A brief history is given elsewhere (Tammann & Reindl 2012b). The physical background is that old, metal-poor stars terminate—independently of mass—their evolution up the red-giant branch by a helium flash in their electron-degenerate cores (see Salaris 2012; and references therein).

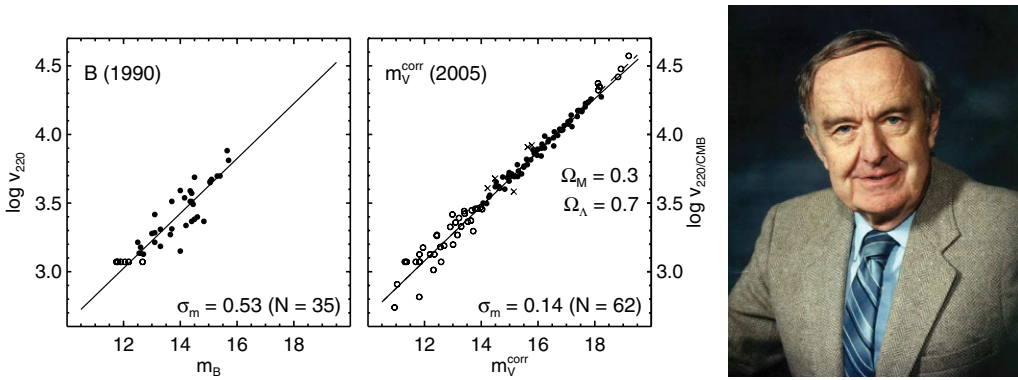


**Figure 6.** (left) Hubble diagram of SNe Ia as of 1990 (Tammann & Leibundgut 1990); it was limited to  $\sim 10,000 \text{ km s}^{-1}$  and had large scatter. (middle) Same, as of 2005 (Reindl *et al.* 2005) out to  $30,000 \text{ km s}^{-1}$ . The 62 SNe Ia with  $3000 < v < 20,000 \text{ km s}^{-1}$  (black dots) have a scatter of only 0.14 mag. The slightly curved Hubble line assumes  $\Omega_M = 0.3$  and  $\Omega_\Lambda = 0.7$ . (right) Allan Sandage in Baltimore (1988).

The TRGB  $I$ -band magnitude,  $M_I^*$ , has exceptionally favorable properties as a distance indicator: its physics is well understood, being observed in outer halo fields it suffers virtually no internal absorption and blends, and as a cut-off magnitude it is free of selection effects; moreover it varies little over a wide metallicity range ( $-2.0 < [\text{Fe}/\text{H}] < -1.2$  dex). The calibration of the TRGB magnitude is very solid. Sakai *et al.* (2004) found  $M_I^* = -4.05$  mag from globular clusters. Rizzi *et al.* (2007) fitted the horizontal branch (HB) of five galaxies to a metal-corrected HB from *Hipparcos* parallaxes and obtained the same value. The 24 galaxies with known RR Lyrae distances and known TRGB magnitudes yield  $M_I^* = -4.05 \pm 0.02$  mag with a dispersion of only 0.08 mag; the underlying RR Lyrae luminosity of  $M_V(\text{RR}) = 0.52$  mag at  $[\text{Fe}/\text{H}] = 1.5$  dex (Sandage & Tammann 2006) is now robustly confirmed by Federici *et al.* (2012). The models of Salaris (2012) also give the same value of  $M_I^*$ . A value of  $M_I^* = -4.05 \pm 0.05$  mag is adopted in the following.

A practical problem of the TRGB as a distance indicator are star fields that do not only contain a predominantly old halo population, but that include also an important fraction of Population I stars. In the latter case, evolved asymptotic giant-branch (AGB) stars and supergiants, which may become as red and even brighter than the TRGB, may swamp the RGB and make the detection of the true TRGB difficult or impossible. Spurious detections are the consequence. The cases of NGC 3368, NGC 3627, and NGC 4038 are discussed in Tammann & Reindl (2012b). While this paper was written, the ambiguity of M101 was solved by Lee & Jang (2012); they determined the TRGB in eight galaxy fields, yielding a high-precision mean apparent magnitude of  $m^* = 25.28 \pm 0.01$  mag.

## 7. The Local Velocity Field

TRGB magnitudes  $m_I^*$  of over 200 galaxies are available in the literature, 190 of them lie outside the Local Group (for a compilation see, e.g., Tammann *et al.* [2008b], with some corrections and additions by various authors). Their distance moduli are derived from the above calibration,  $M_I^* = -4.05$  mag, and are expressed as distance moduli  $(m - M)^{00}$  from the barycenter of the Local Group, assumed to lie two thirds of the way toward M31. The 190 galaxies are plotted in a Hubble diagram in Fig. 7. The velocities

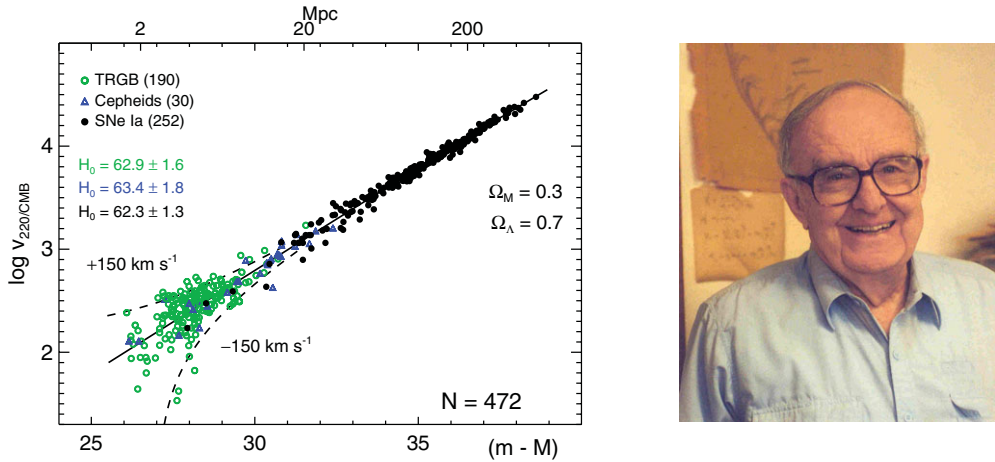


**Figure 7.** (left) Distance-calibrated Hubble diagram showing distance moduli from the TRGB (green open circles), Cepheids (blue triangles), and SNe Ia (black dots). The slightly curved Hubble line holds for a model with  $\Omega_M = 0.3$ ,  $\Omega_\Lambda = 0.7$ . The envelopes for peculiar velocities of  $\pm 150 \text{ km s}^{-1}$  are shown as dashed lines. (right) Allan Sandage in front of his CMD of open clusters, ca. 1990.

$v_{220}$  are corrected for a self-consistent Virgocentric infall model with a local infall vector of  $220 \text{ km s}^{-1}$  and a density profile of the Local Supercluster of  $\rho \sim r^{-2}$  (Yahil *et al.* 1980); the correction  $\Delta v_{\text{Virgo}}$  follows then from eq. (5) in Sandage *et al.* (2006).

The scatter in Fig. 7 increases with decreasing distance as a result of the peculiar velocities of individual galaxies, of order  $50\text{--}70 \text{ km s}^{-1}$ . An excess of slow galaxies at very short distances is obviously the result of the pull from the Local Group. The 79 TRGB galaxies with  $(m - M) > 28.2$  mag define a Hubble line with slope  $0.199 \pm 0.019$ , in agreement with a locally constant expansion rate. The mean value of  $H_0$  is well-defined at  $62.9 \pm 1.6 \text{ km s}^{-1} \text{ Mpc}^{-1}$  (statistical error) at a median velocity of  $v_{220} = 350 \text{ km s}^{-1}$ .

Also plotted in Fig. 7 are 34 galaxies (outside the Local Group) with Cepheid distances from Saha *et al.* (2006). The 30 galaxies with  $(m - M) > 28.2$  mag yield the expected Hubble line slope of  $0.200 \pm 0.010$  and a mean value of  $H_0 = 63.4 \pm 1.8 \text{ km s}^{-1} \text{ Mpc}^{-1}$  at a median velocity of  $v_{220} = 900 \text{ km s}^{-1}$ .

In addition, Fig. 7 shows 252 SNe Ia with known maximum magnitudes  $m_V^{\text{corr}}$  in the system of Reindl *et al.* (2005) and with  $v < 30,000 \text{ km s}^{-1}$ . Their moduli follow from the calibration  $M_V^{\text{corr}} = -19.46$  mag in Section 5. The 190 SNe Ia within  $3000 < v < 20,000 \text{ km s}^{-1}$  fit the Hubble line for  $\Omega_M = 0.3$  and  $\Omega_\Lambda = 0.7$  with a scatter of only 0.15 mag. The SNe Ia give a large-scale value of  $H_0 = 62.3 \text{ km s}^{-1} \text{ Mpc}^{-1}$ , i.e. the same as the more restricted SN sample in Section 5.

The agreement within statistics of  $H_0$  from Cepheids and SNe Ia is by construction, because the SN luminosities are calibrated by means of a subsample of these Cepheids. However, the close agreement of  $H_0$  from Cepheids and SNe Ia with the mean value of  $H_0$  from local and *independent* TRGB distances is highly significant, indicating that any change in  $H_0$  is undetectable over a range as wide as  $300 < v < 30,000 \text{ km s}^{-1}$ . An equivalent conclusion can be drawn also without any absolute distance scale, because TRGBs, Cepheids, and SNe Ia have sufficient redshift overlap to smoothly connect the three segments of the Hubble line into a single line. This limits the change of  $H_0$  to 4% over the entire distance range (Tammann & Reindl 2012a).

The data sets in Fig. 7 are well suited to shed some light on the motion of the Local Volume causing the cosmic microwave background (CMB) dipole. Once the observed

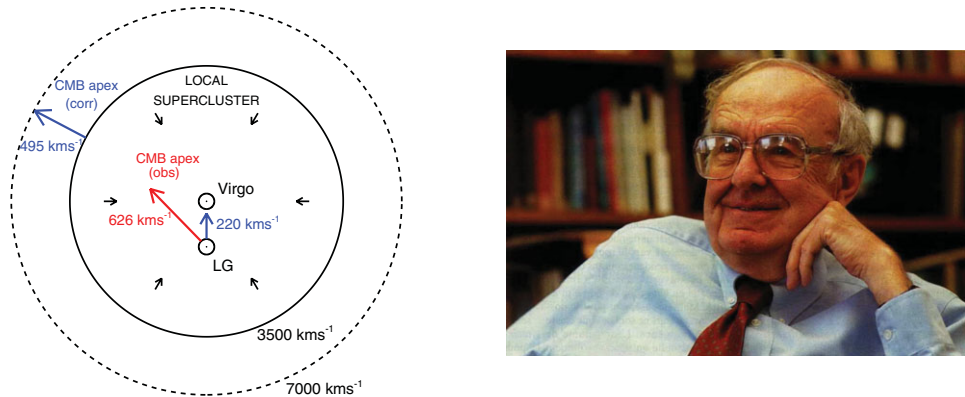


**Figure 8.** (left) Schematic view of the Local Supercluster with the Virgo cluster at its center. The off-center Local Group (LG) is shown with its Virgo-centric infall vector. The observed local velocity vector relative to the CMB is shown as well as the bulk motion, corrected for the Virgo-centric infall vector, of the Local Supercluster toward the corrected apex  $A_{\text{corr}}$ . (right) Allan Sandage in 1998. (Photo: *Ciel et Espace*)

apex velocity and direction (Hinshaw *et al.* 2007) are corrected for the local Virgo-centric infall vector of  $220 \text{ km s}^{-1}$ , one obtains a predicted non-Hubble velocity of  $495 \pm 25 \text{ km s}^{-1}$  in the direction of a corrected apex  $A_{\text{corr}}$  at  $l = 275 \pm 2$ ,  $b = 12 \pm 4$  degrees in the constellation of Vela (Fig. 8; see also Sandage & Tammann 1984). The question is how large is the co-moving volume of the Local Supercluster? An answer is given in Fig. 9, where the residuals  $\Delta v_{220}$  from the Hubble line in Fig. 7 are plotted against  $\cos(\alpha)$ ;  $\alpha$  is the angle between a given object and  $A_{\text{corr}}$ . The flat distribution of the objects with  $500 < v_{220} < 3500 \text{ km s}^{-1}$  in Fig. 9a rules out any systematic motion toward  $A_{\text{corr}}$  within the Local Supercluster. In sharp contrast, objects with  $3500 < v_{220} < 7000 \text{ km s}^{-1}$  reveal (in Fig. 9b) a highly significant (three-dimensional) velocity of  $448 \pm 73 \text{ km s}^{-1}$  in the direction of  $A_{\text{corr}}$  and in statistical agreement with the predicted value of  $495 \pm 25 \text{ km s}^{-1}$ . The emerging picture is that the Local Supercluster is a contracting entity, as strongly suggested by the local Virgo-centric infall, which moves in bulk motion relative to the objects in a shell between  $3500$  and  $7000 \text{ km s}^{-1}$ , constituting the Machian frame. The acceleration of the Local Supercluster must be caused by the irregular mass and void distribution within this shell. The role of the Great Attractor as accelerator is not clear; it lies with  $v \sim 4700 \text{ km s}^{-1}$  in the expected distance range, but  $40^\circ$  away from  $A_{\text{corr}}$ . In any case, Shapley's Supercluster at  $50^\circ$  from  $A_{\text{corr}}$  and at  $v \sim 13,000 \text{ km s}^{-1}$  is too distant to contribute noticeably to the acceleration of the Local Supercluster.

All galaxies with  $v_{220} > 3500 \text{ km s}^{-1}$  have been corrected in this paper by  $\Delta v_{\text{CMB}} = 495 \cos(\alpha)$  to compensate for the motion of the Local Supercluster relative to the CMB.

## 8. The Luminosity Calibration of SNe Ia from the TRGB

The first attempts to calibrate the SNIa luminosity based upon TRGB distances are from Tammann *et al.* (2008a) and Mould & Sakai (2009). Then a year ago, and two years after Allan Sandage's death, the Stone of Rosetta appeared in the form of the unreddened *standard* SNIa 2011fe (Nugent *et al.* 2011) in M101 with a firm TRGB distance (see Sect. 6). This brings the number of SNIa with known TRGB distances to six, which forms a solid basis for a luminosity calibration of SNe Ia. The SNe Ia are individually discussed elsewhere (Tammann & Reindl 2012b); their relevant parameters (including the revised TRGB distance of M101 in Sect. 6) and their compounded statistical errors are

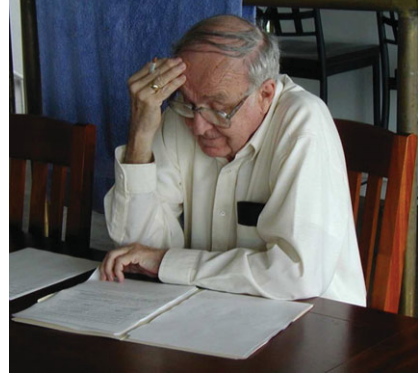
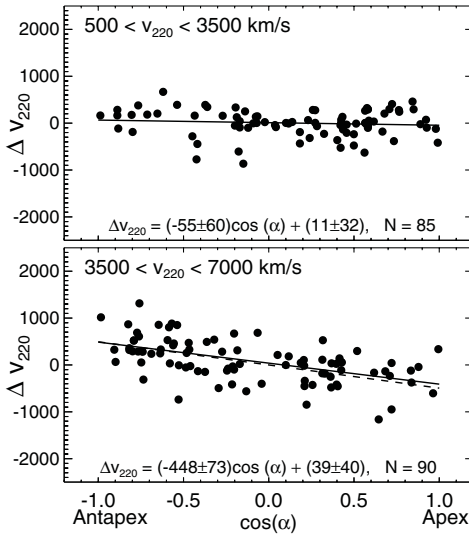


**Figure 9.** (left) The velocity residuals  $\Delta v_{220}$  from the Hubble line in Fig. 7, shown as a function of  $\cos(\alpha)$ , where  $\alpha$  is the angle between the object and the corrected CMB apex  $A_{\text{corr}}$ , (a) for objects with  $500 < v_{220} < 3500 \text{ km s}^{-1}$ , and (b) for objects with  $3500 < v_{220} < 7000 \text{ km s}^{-1}$ . (right) Allan Sandage in 2002.

**Table 1.** The TRGB calibration of SNe Ia

SN (1)	Galaxy (2)	$m_V^{\text{corr}}$ (3)	$(m-M)_{\text{TRGB}}$ (4)	Ref. (5)	$M_V^{\text{corr}}$ (6)
2011fe	NGC 5457	9.93 (06)	29.33 (02)	1	-19.40 (06)
2007sr	NGC 4038	12.26 (13)	31.51 (12)	2	-19.25 (18)
1998bu	NGC 3368	11.01 (12)	30.39 (10)	3	-19.38 (16)
1989B	NGC 3627	10.94 (11)	30.39 (10)	3	-19.45 (15)
1972E	NGC 5253	8.37 (11)	27.79 (10)	4,5	-19.42 (15)
1937C	IC 4182	8.92 (16)	28.21 (05)	4,5	-19.29 (17)
straight mean					$-19.37 \pm 0.03$
weighted mean					$-19.39 \pm 0.05$

(1) Lee & Jang 2012; (2) Schweizer *et al.* 2008; (3) galaxy assumed at the mean TRGB distance of the Leo I group; (4) Sakai *et al.* 2004; (5) Rizzi *et al.* 2007.

compiled in Table 1. Their resulting weighted mean luminosity of  $M_V^{\text{corr}} = -19.39 \pm 0.05$  mag, inserted in Eq. (5.1), yields

$$H_0 = 64.6 \pm 1.6 \pm 2.8 \text{ km s}^{-1} \text{ Mpc}^{-1}, \quad (8.1)$$

where the systematic error is justified in Tammann & Reindl (2012b).

Cepheid distances are available for all six SNe Ia in Table 1; they yield  $M_V^{\text{corr}} = -19.40 \pm 0.06$  mag (Tammann & Reindl 2012b, their table 3), in fortuitous agreement with the TRGB calibration. Additional weight to the present calibration is given by two galaxies in the Fornax Cluster that have produced four SNe Ia (SNe 1980N, 1981D, 1992A, and 2006dd) and whose surface brightness fluctuation (SBF) distances from *HST*/ACS are given by Blakeslee *et al.* (2010); they lead, again independently, to a weighted mean value of  $M_V^{\text{corr}} = -19.43 \pm 0.06$  mag.

## 9. Results and Conclusions

The large-scale value of  $H_0$  is provided by the Hubble diagram of SNe Ia with  $3000 < v < 20,000 \text{ km s}^{-1}$  (and beyond) pending the calibration of their absolute magnitude and its error. Two nearby calibrations based on young Population I (Cepheids) and old Population II (TRGB) distance indicators lead, in good agreement, to a weighted mean SN Ia luminosity of  $M_V^{\text{corr}} = -19.41 \pm 0.04 \text{ mag}$ . The result is further and independently supported by four SNe Ia in two Fornax galaxies with modern SBF distances. A combination of the adopted calibration with Eq. (5.1) leads therefore to a firm cosmic value of the Hubble constant of  $H_0 = 64.1 \pm 2.4 \text{ km s}^{-1} \text{ Mpc}^{-1}$  (systematic error included).

The calibrated SNe Ia are well suited to assess the distances to many galaxies (e.g., Tammann *et al.* 2008b), and particularly to clusters with multiple occurrences. Prime example is the Fornax Cluster, with five SNe Ia (as above as well as SN 2001el) that give—with  $\langle m_V^{\text{corr}} \rangle = 12.19 \pm 0.09 \text{ mag}$ —a distance of  $(m - M)^{00} = 31.60 \pm 0.10 \text{ mag}$  ( $H_{\text{Fornax}} = 66 \pm 4 \text{ km s}^{-1} \text{ Mpc}^{-1}$ ), in good agreement with the entirely independent mean SBF cluster distance modulus of  $31.55 \pm 0.04 \text{ mag}$  (Blakeslee *et al.* 2010). The Virgo Cluster would need more than its present four SNe Ia for a good distance determination because of its important depth effect. The best value of  $(m - M) = 31.18 \pm 0.10 \text{ mag}$  ( $(m - M)^{00} = 31.22 \pm 0.10 \text{ mag}$ ;  $H_{\text{Virgo}} = 66 \pm 5 \text{ km s}^{-1} \text{ Mpc}^{-1}$ ) comes from the difference between Fornax and Virgo of  $\Delta(m - M) = 0.42 \pm 0.02 \text{ mag}$ , based on a wealth of SBF distances (Blakeslee, this volume).

A promising development is the extension of water megamaser distances out to  $\sim 10,000 \text{ km s}^{-1}$ . So far, four sources yield  $H_0 = 70.5 \pm 5.4 \text{ km s}^{-1} \text{ Mpc}^{-1}$  (Braatz, this volume), which is statistically not excluded by the value derived here. Yet, at least in one case, the value of  $H_0$  depends heavily on the  $H_0$  prior chosen (Reid *et al.* 2012b).

For values of  $H_0$  from strong gravitational lenses and from the Sunyaev–Zel’dovich effect, both quite model-dependent, the reader is referred to Suyu (this volume) and Bonamente (this volume), respectively.

The CMB fluctuation spectrum (*imprinted at an early epoch*) has led to many estimates of the (*present*) value of  $H_0$ , but they are necessarily model-dependent and rely on a variety of free parameters and, in some cases, on the choice of priors. Komatsu *et al.* (2011) derived, from a simple six-parameter analysis of the WMAP7 data,  $H_0 = 70.3 \text{ km s}^{-1} \text{ Mpc}^{-1}$ , yet imposing a prior  $H_0 = 74.2 \pm 3.6 \text{ km s}^{-1} \text{ Mpc}^{-1}$ . Other authors have included additional evidence from large red galaxies, the shape of the Hubble diagram of SNe Ia, and from baryon acoustic oscillations (BAO); their results cluster around  $H_0 = 69 \text{ km s}^{-1} \text{ Mpc}^{-1}$  (Anderson *et al.* 2012; Reid *et al.* 2012a; Sánchez *et al.* 2012).

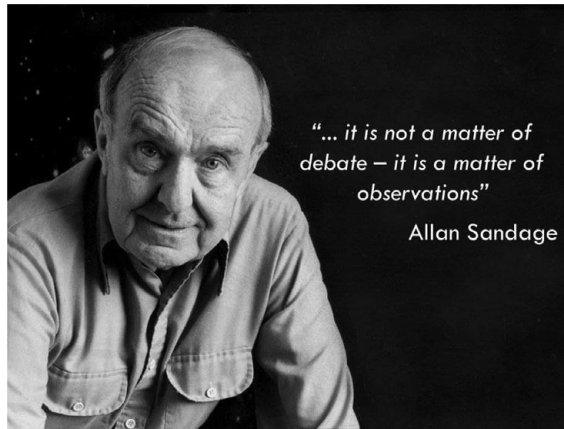
Calabrese *et al.* (2012) analyzed the WMAP7 data, combined with ground-based observations on arcminute angular scales, making different model assumptions. If they impose the standard value of  $N_{\text{eff}} = 3.046$  for the number of effective relativistic neutrinos and set a prior of  $H_0 = 68 \pm 2.8 \text{ km s}^{-1} \text{ Mpc}^{-1}$ , they find  $H_0 = 66.8 \pm 1.8 \text{ km s}^{-1} \text{ Mpc}^{-1}$ . In case of non-standard decoupling of neutrinos, the value could be lower (A. Melchiorri, priv. commun.).

Of particular interest is the BAO peak found in the correlation function of the 6dF Galaxy Survey at a redshift of  $z = 0.106$ , the lowest redshift so far (Beutler *et al.* 2011; Colless, this volume). This allows the authors to evaluate  $H_0$ , making minimum use of CMB data. Their result of  $H_0 = 67 \pm 3.2 \text{ km s}^{-1} \text{ Mpc}^{-1}$  does not yet decide between the present result and  $H_0 \sim 70 \text{ km s}^{-1} \text{ Mpc}^{-1}$ , but it makes still higher values in the literature less probable. Tighter constraints are foreseeable.

Sandage’s last published value of the Hubble constant is  $H_0 = 62.3 \text{ km s}^{-1} \text{ Mpc}^{-1}$  (Tammann & Sandage 2010). This value has been slightly revised to  $H_0 = 64.1 \pm 2.4$

km s<sup>-1</sup> Mpc<sup>-1</sup> to account for the high-weight TRGB calibration of SNe Ia. If confirmed, the value will be useful to constrain some of the fundamental parameters of the Universe.

*Dedication:* To the memory of a great man, Allan Sandage.



## References

- Anderson, L., Aubourg, E., Bailey, S., *et al.* 2012, arXiv:1203.6594
- Baade, W. 1944, *ApJ*, 100, 137
- Baade, W. 1948, *PASP*, 60, 230
- Baade, W. & Swope, H. H. 1963, *AJ*, 68, 435
- Beutler, F., Blake, C., Colless, M., *et al.* 2011, *MNRAS*, 416, 3017
- Blakeslee, J. P. 2012, *Ap&SS*, 341, 179
- Blakeslee, J. P., Cantiello, M., Mei, S., *et al.* 2010, *ApJ*, 724, 657
- Bresolin, F. 2011, *ApJ*, 729, 56
- Burbidge, G. R., Burbidge, E. M., & Sandage, A. 1963, *Rev. Mod. Phys.*, 35, 947
- Calabrese, E., Archidiacono, M., Melchiorri, A., & Ratra, B. 2012, *Phys. Rev. D*, 86, 043520
- de Vaucouleurs, G. & Peters, W. L. 1985, *ApJ*, 297, 27
- Eggen, O. J., Lynden-Bell, D., & Sandage, A. 1962, *ApJ*, 136, 748
- Federici, L., Cacciari, C., Bellazzini, M., Fusi Pecci, F., Galletti, S., & Perina, S. 2012, *A&A*, 544, A155
- Freedman, W. L., Madore, B. F., Gibson, B. K., *et al.* 2001, *ApJ*, 553, 47
- Hicken, M., Wood-Vasey, W. M., Blondin, S., *et al.* 2009, *ApJ*, 700, 1097
- Hinshaw, G., Nolta, M. R., Bennett, C. L., *et al.* 2007, *ApJ*, 170, 288
- Humason, M. L., Mayall, N. U., & Sandage, A. R. 1956, *AJ*, 61, 97
- Kessler, R., Becker, A. C., Cinabro, D., *et al.* 2009, *ApJ*, 185, 32
- Komatsu, E., Smith, K. M., Dunkley, J., *et al.* 2011, *ApJ*, 192, 18
- Kudritzky, R. P. & Urbaneja, M. A. 2012, *Ap&SS*, 341, 131
- Lee, M. G., Freedman, W. L., & Madore, B. F. 1993, *ApJ*, 417, 553
- Lee, M. G. & Jang, I. S. 2012, *ApJ*, 760, L14
- Mould, J. & Sakai, S. 2009, *ApJ*, 697, 996
- Nugent, P. E., Sullivan, M., Cenko, S. B., *et al.* 2011, *Nature*, 480, 344
- Phillips, M. M. 1993, *ApJ*, 413, L105
- Reid, B. A., Samushia, L., White, M., *et al.* 2012a, *MNRAS*, 426, 2719
- Reid, M. J., Braatz, J. A., Condon, J. J., Lo, K. Y., Kuo, C. Y., Impellizzeri, C. M. V., & Henkel, C. 2012b, *ApJ*, submitted (arXiv:1207.7292)
- Reindl, B., Tammann, G. A., Sandage, A., & Saha, A. 2005, *ApJ*, 624, 532
- Riess, A. G., Macri, L., Casertano, S., *et al.* 2011, *ApJ*, 730, 119

- Rizzi, L., Tully, R. B., Makarov, D., *et al.* 2007, *ApJ*, 661, 815
- Saha, A., Thim, F., Tammann, G. A., Reindl, B., & Sandage, A. 2006, *ApJ*, 165, 108
- Sakai, S., Ferrarese, L., Kennicutt, R. C., & Saha, A. 2004, *ApJ*, 608, 42
- Salaris, M. 2012, *Ap&SS*, 341, 65
- Sánchez, A. G., Scoccola, C. G., Ross, A. J., *et al.* 2012, *MNRAS*, 425, 415
- Sandage, A. 1953, *AJ*, 58, 61
- Sandage, A. 1958a, *ApJ*, 127, 513
- Sandage, A. 1958b, *Recherche Astronomique*, 5, 41
- Sandage, A. 1961, *ApJ*, 133, 355
- Sandage, A. 1962a, *ApJ*, 136, 319
- Sandage, A. 1962b, in: *Problems of Extra-Galactic Research* (McVittie, G.C., ed.), Proc. IAU Symp. 15, p. 359
- Sandage, A. 1970, *Phys. Today*, 23(2), 34
- Sandage, A. 1972, *QJRAS*, 13, 282
- Sandage, A. 1975, *ApJ*, 202, 563
- Sandage, A. 1986, in: *Star-forming dwarf galaxies and related objects* (Kunth, D., Thuan, T. X., & Trần Thanh Vân, J., eds.), Gif-sur-Yvette: Ed. Frontières, p. 31
- Sandage, A. 2000, *PASP*, 112, 504
- Sandage, A. 2004, *The Mount Wilson Observatory*, Cambridge: Cambridge Univ. Press
- Sandage, A. 2010, *AJ*, 139, 728
- Sandage, A., Bell, R. A., & Tripicco, M. J. 1999, *ApJ*, 522, 250
- Sandage, A., Binggeli, B., & Tammann, G. A. 1985, *AJ*, 90, 1759
- Sandage, A., Reindl, B., & Tammann, G. A. 2010, *ApJ*, 714, 1441
- Sandage, A. & Schwarzschild, M. 1952, *ApJ*, 111, 463
- Sandage, A. & Tammann, G. A. 1968, *ApJ*, 151, 531
- Sandage, A., & Tammann, G.A. 1974–1975, *ApJ*, 190, 525; 191, 603; 194, 223; 194, 559; 196, 313; 197, 265
- Sandage, A. & Tammann, G. A. 1982, *ApJ*, 256, 339
- Sandage, A. & Tammann, G. A. 1984, in: *Large-Scale Structure of the Universe, Cosmology and Fundamental Physics* (Setti, G., & van Hove, L., eds.), Garching: ESO, p. 127
- Sandage, A. & Tammann, G. A. 2006, *ARA&A*, 44, 93
- Sandage, A., Tammann, G. A., & Federspiel, M. 1995, *ApJ*, 452, 1
- Sandage, A., Tammann, G. A., & Hardy, E. 1972, *ApJ*, 172, 253
- Sandage, A., Tammann, G. A., Saha, A., Reindl, B., Macchetto, F. D., & Panagia, N. 2006, *ApJ*, 653, 843
- Schweizer, F., Burns, C. R., Madore, B. F., *et al.* 2008, *AJ*, 136, 1482
- Shappee, B. J., & Stanek, K. Z. 2011, *ApJ*, 733, 124
- Tammann, G. A. & Leibundgut, B. 1990, *A&A*, 236, 9
- Tammann, G. A. & Reindl, B. 2012a, *Ap&SS*, 341, 3
- Tammann, G. A. & Reindl, B. 2012b, *A&A*, arXiv:1208.5054
- Tammann, G. A., Reindl, B., & Sandage, A. 2011, *A&A*, 531, 134
- Tammann, G. A. & Sandage, A. 1968, *ApJ*, 151, 825
- Tammann, G. A. & Sandage, A. 2010, in: *The Impact of HST on European Astronomy* (Macchetto, F.D., ed.), Astrophys. Space Sci. Proc., Dordrecht: Springer, p. 289
- Tammann, G. A., Sandage, A., & Reindl, B. 2008a, *ApJ*, 679, 52
- Tammann, G. A., Sandage, A., & Reindl, B. 2008b, *A&ARev*, 15, 289
- van den Bergh, S. 1960, *Publ. David Dunlap Obs.*, 2, 159
- Yahil, A., Sandage, A., & Tammann, G. A. 1980, *ApJ*, 242, 448
- Zwicky, F., *et al.* 1961–1968, *Catalogue of galaxies and of clusters of galaxies, Vol. I–VI*, Pasadena: California Institute of Technology